

# THE LUNAR ICECUBE MISSION CHALLENGE: ATTAINING SCIENCE ORBIT PARAMETERS FROM A CONSTRAINED APPROACH TRAJECTORY

David C. Folta<sup>\*</sup>, Natasha Bosanac<sup>†</sup>, Andrew Cox<sup>‡</sup>, and Kathleen C. Howell<sup>§</sup>

The challenges of targeting specific lunar science orbit parameters from a concomitant Sun-Earth/Moon system trajectory are examined. While the concept of ballistic lunar capture is well-studied, achieving and controlling the time evolution of the orbital elements to satisfy mission constraints is especially problematic when the spacecraft is equipped with a low-thrust propulsion system. Satisfying these requirements on the lunar approach and capture segments is critical to the success of the Lunar IceCube mission, a 6U CubeSat that will prospect for water in solid (ice), liquid, and vapor forms and other lunar volatiles from a low-periapsis, highly inclined elliptical lunar orbit.

## INTRODUCTION

Injected into a direct lunar transfer as a payload onboard Exploration Mission-1 (EM-1) on the initial flight of NASA's Space Launch System (SLS), Lunar IceCube will employ a lunar gravity assisted multi-body transfer trajectory with an innovative RF Ion engine to return to the Moon and attain a specific lunar science orbit. Constraints on the translunar trajectory limit the types of feasible Sun-Earth/Moon transfers which encounter the Moon with the necessary ballistic capture energy and orbit orientation. For Lunar IceCube, key dynamical parameter values must be attained to enable the ballistically captured trajectory to evolve into the desired science orbit. If these parameter values are not achieved during this lunar approach phase, gravitational perturbations may result either in lunar impact or in a captured orbit that does not meet the mission requirements and cannot be sufficiently altered given the limitations of the propulsion system. However, dynamical systems analysis demonstrates that capture dynamics can lead to stable trajectories that remain bounded around the Moon. This paper addresses the subsequent challenge of achieving a desired set of orbital elements prior to the science phase of the mission.

In this investigation, a trajectory design strategy is offered for achieving and maintaining a lunar orbit that satisfies the mission requirements, subject to significant propulsive limitations. Development of these procedures leverages analyses of the Earth-Moon dynamics via mapping techniques, orbital evolution predictions, and numerical simulations. The resulting strategies reveal that the geometry and availability of feasible lunar approach and capture arcs is impacted by: 1) the

---

<sup>\*</sup> Senior Fellow, NASA Goddard Space Flight Center, Greenbelt, Maryland 20771, USA.

<sup>†</sup> Post-Doctoral Research Assistant, School of Aeronautics and Astronautics, Purdue University, 701 W. Stadium Ave., West Lafayette, Indiana 47907, USA; currently Assistant Professor, Department of Aerospace Engineering Sciences, University of Colorado Boulder, 429 UCB, Boulder, Colorado 80309, USA.

<sup>‡</sup> Graduate Student, School of Aeronautics and Astronautics, Purdue University, 701 W. Stadium Ave., West Lafayette, Indiana 47907, USA.

<sup>§</sup> Hsu Lo Distinguished Professor of Aeronautics and Astronautics, School of Aeronautics and Astronautics, Purdue University, 701 W. Stadium Ave., West Lafayette, Indiana 47907, USA.

evolution of low lunar orbits subject to gravitational and other perturbations, as well as 2) constraints on the EM-1 deployment conditions and, therefore, the lunar arrival trajectory. To perform this analysis, Purdue University's Adaptive Trajectory Design (ATD) dynamical systems software, NASA Goddard Space Flight Center's General Mission Analysis Tool (GMAT) and AGI's STK Astrogator tool are employed. While the strategy for designing a capture trajectory is demonstrated for the Lunar IceCube mission, the general procedure may also be applicable to other lunar missions that possess similar limitations on the maneuver control authority.

## **CubeSats and Constrained Transfer Trajectories**

The miniaturization of spacecraft technologies and launch availability as secondary payloads offer a significantly reduced cost and development time over conventional, larger spacecraft. These small spacecraft, such as CubeSats, benefit public and private entities as well as educational institutions. Currently, thirteen CubeSats are intended to launch onboard the second stage of the Exploration Mission-1 vehicle (EM-1).<sup>1</sup> Following injection into a translunar trajectory, each secondary payload is deployed and then must navigate to various destinations by leveraging natural dynamics along with the use of onboard propulsion. These missions will achieve various scientific and technology demonstration objectives, such as testing solar sail technology, investigating near-Earth asteroids, surveying the Moon for water ice, and measuring the effects of deep-space radiation on living organisms.<sup>2</sup>

Missions involving spacecraft that are contingent upon an independent launch opportunity to attain a desired transfer trajectory or science orbit face numerous trajectory design challenges. For these spacecraft, a fixed departure asymptote and translunar energy value limit the design space for transfer trajectories and achievable science orbits. Furthermore, CubeSats typically incorporate small propulsion systems that possess limited thrusting capabilities. The inherent uncertainty associated with both the launch date and the deployment state for secondary payloads, as well as low thrust levels, can affect both the scope and capability of a CubeSat mission, and pose significant challenges for trajectory design.

Trajectory design challenges are not unique to CubeSats; many other spacecraft face similar constraints during extended mission phases when propellant reserves are low or following subsystem failures that affect a vehicle's ability to maneuver. Consider, for example, the Acceleration, Reconnection, Turbulence and Electrodynamics of the Moon's Interaction with the Sun (ARTEMIS) mission, which repurposed two Time History of Events and Macroscale Interactions during Substorms (THEMIS) vehicles for an extended mission to the Earth-Moon  $L_1$  and  $L_2$  regions.<sup>3</sup> Since neither spacecraft possessed sufficient propellant to implement a direct injection, a series of gravity assists were leveraged to reach transfer paths identified via dynamical systems theory. In addition to identifying low-cost transfer options, dynamical systems analysis affords insight into the flow near a particular solution, which provides alternative options and facilitates design flexibility to deal with uncertainties and operational errors.

Designing attainable trajectories that can achieve complex scientific goals for CubeSats with limited propulsive capability is challenging and requires an understanding of the dynamical structure to determine the overall bounding conditions and the natural (predictable) motion. In this investigation, dynamical models of varying levels of fidelity are leveraged to construct a preliminary trajectory design framework for the attainment of specific lunar orbit parameter values. These parameter values are then employed in higher fidelity operational tools to complete the design process and are applied to the upcoming Lunar IceCube mission, which must reach a lunar orbit for scientific observation of the Moon's equatorial regions. Despite an energetic initial deployment state as a secondary payload, Lunar IceCube can achieve the desired final science orbit by exploiting the dynamics of the Sun-Earth and Earth-Moon system. The Circular Restricted Three-Body Problem (CR3BP) is employed to quickly assess the process. In this autonomous

dynamical model, approximate bounds on the motion are established and capture geometries can be understood via manifolds associated with libration point orbits, gateway dynamics and the Jacobi constant. This analysis is then transitioned to a higher-fidelity ephemeris model that also includes the additional contribution of a low-thrust engine. Boundary conditions such as the initial deployment state and the final science orbit parameters are incorporated into this trajectory design framework to identify lunar arrival regions and geometries that correspond to feasible transfer trajectories for the Lunar IceCube mission.

## THE LUNAR ICECUBE MISSION

Lunar IceCube, a 6U CubeSat, has been selected for participation in the Next Space Technologies for Exploration Partnerships, which leverages partnerships between public and private entities to develop the deep space exploration capabilities necessary for the next steps in human spaceflight.<sup>4,5</sup> The Lunar IceCube mission is led by the Space Science Center at Morehead State University (MSU) and is supported by scientists and engineers from NASA Goddard Spaceflight Center (GSFC), Busek Co., JPL, and Catholic University of America (CUA). Specifically, GSFC is providing the trajectory design, maneuver planning, navigation and tracking support, and attitude support.

The primary objective for the Lunar IceCube mission is to prospect for water in solid, liquid and vapor forms, while also detecting other lunar volatiles. Accordingly, this mission is designed to address existing strategic knowledge gaps related to lunar volatile distribution, focusing on the abundance, location and transportation physics of water ice on the lunar surface at a variety of latitudes. The required scientific observations will be performed from a highly-inclined, low-periapsis, elliptical lunar orbit using the Broadband InfraRed Compact High Resolution Exploration Spectrometer (BIRCHES). The BIRCHES instrument is designed specifically for CubeSats by GSFC as a compact version of the Origins, Spectral Interpretation, Resource Identification, Security - Regolith Explorer (OSIRIS-REx) Visible and Infrared Spectrometer as well as the Ralph spectrometer that was successfully used onboard the New Horizons mission. The design of the Lunar IceCube spacecraft, illustrated in Figure 1, also includes radiation-hardened subsystems, a JPL Iris transceiver, a high power solar panel/actuator system and a robust multiple-processor based payload processor. These systems will enable the spacecraft to perform scientific observations for approximately six months, enabling sufficient collection of systematic volatile measurements to derive volatile cycle models. Science data and telemetry will be transmitted from the lunar vicinity at a rate of 128 Kbps to the controlling 21-meter ground station at MSU. The MSU antenna will also be used as the primary command and tracking station during the propulsion phase of the mission and will be used for ranging and tracking.



**Figure 1. Lunar IceCube spacecraft design.**

Lunar IceCube will ride onboard the EM-1 vehicle, currently scheduled for launch in late 2018. Each of the secondary payloads are deployed after Orion is injected and the Interim Cryogenic Propulsion Stage (ICPS) disposal maneuver is completed. Due to uncertainties in the ejection mechanism, Lunar IceCube's exact deployment state is not known in advance. However, with no additional maneuvers, the highly energetic nominal deployment state would result in the spacecraft

quickly departing the Earth-Moon system. To decrease the spacecraft energy and achieve a transfer that approaches a low-periapsis lunar orbit, the Lunar IceCube spacecraft is equipped with a low-thrust propulsion system. This iodine-fueled engine is a Busek Ion Thruster 3-cm (BIT-3) system, which is currently designed to deliver a maximum 1.15mN of thrust with an  $I_{sp}$  of 2500s and a fuel mass of approximately 1.5 kg.<sup>6</sup> For the Lunar IceCube mission, the BIT-3 system enables finite duration low-thrust arcs to be introduced along the transfer trajectory.

The final lunar science orbit is constrained to meet requirements imposed by the science instruments. The BIRCHES instrument requires that observations be performed from an elliptical orbit to minimize thermal exposure, with an equatorial perilune altitude of 100 to 105 km. This science orbit is designed to be inertially-locked to allow measurement of lunar volatiles for the same set of representative features (by latitude, composition and age of regolith) at various times during the day. In this science orbit, the BIRCHES adjustable iris allows the instrument to act as a point spectrometer with constant footprint dimensions that are independent of the distance from the lunar surface, as the spacecraft altitude varies in orbit from 100 to 250 km, i.e., from periapsis to the terminator. The spacecraft ACS system will allow the BIRCHES instrument to maintain lunar nadir-pointing during science passes.

## **DYNAMICAL MODELS AND TECHNIQUES**

To explore the design space for low-thrust enabled transfers that link an arrival trajectory with the lunar science orbit, dynamical models of varying levels of fidelity are employed: from the CR3BP to an operational modeling environment.<sup>11</sup> The CR3BP offers an autonomous model of the Earth-Moon system which admits a constant, energy-like integral labeled the Jacobi constant,  $C = 2U - \dot{x}^2 - \dot{y}^2 - \dot{z}^2$ . This simplified dynamical model enables the development of a general itinerary for the Lunar IceCube spacecraft, the visualization of solutions of interest, and guidance of the process to locate science orbit approach paths. This insight, in combination with techniques from dynamical systems theory, is incorporated into a general procedure for generating feasible trajectories that reach the desired science orbit in a low-thrust-enabled point mass ephemeris model.<sup>11</sup> In this model, the low-thrust engine is parameterized using a constant thrust magnitude, equal to 0.9 mN and a specific impulse of 2500s. In this investigation, the resulting equations of motion are formulated relative to the Moon, with the position coordinates of the Moon, Earth and Sun retrieved from the Jet Propulsion Laboratory DE421 ephemerides. Relative nondimensional coordinates are then used to integrate the motion of a spacecraft relative to the Moon in the low-thrust-enabled four-body point mass ephemeris model via ATD, GMAT, and STK.<sup>7,8,9</sup>

## **TRAJECTORY DESIGN CHALLENGES**

Additional analysis by the authors has demonstrated a process that permits an analyst to design a transfer trajectory from a constrained outbound asymptote to return to the lunar vicinity months later and capture into a lunar orbit.<sup>5,10,11</sup> This trajectory design framework leverages information from the EM-1 mission that will test the SLS performance and the Orion trajectory. The post deployment EM-1 trajectory, augmented by the low-thrust engine of the Lunar IceCube spacecraft, results in a trailing edge lunar gravity assist. By leveraging knowledge of the dynamical systems properties of both Sun-Earth and Earth-Moon systems, the post-deployment conditions are targeted to ensure that the spacecraft returns to the lunar vicinity. In this investigation, this previously-developed transfer design process is implemented in a high fidelity model to produce an operationally feasible trajectory.<sup>10,11</sup>

Given a trajectory that returns to the lunar vicinity, a significant challenge in the design process is obtaining a specific, increasingly stable polar lunar orbit via a low-thrust-enabled path that evolves under the gravitational acceleration of the Earth, Moon, and Sun. The available thrust magnitude is approximately 0.9 mN with a spacecraft mass at lunar arrival between 13 kg and 14

kg, depending on the total thrust time along the reference path as well as the impact of launch error corrections on propellant usage. Upon arriving into the lunar vicinity, a feasible trajectory should deliver the Lunar IceCube spacecraft into a stable elliptical orbit ( $a = 4287\text{km}$ ,  $e = 0.5714$ ) with a near polar inclination and periapsis located over the equator. In the chaotic and nonlinear dynamical environment of the Earth, Moon and Sun, there may be infinite possibilities for achieving the desired science orbit upon arriving into the lunar vicinity. However, the goal of this investigation is to provide guidelines for one possible trajectory design strategy that delivers the spacecraft to the desired orbit subject to the associated operational constraints.

### Sample Lunar IceCube Transfer

One of the primary Lunar IceCube design challenges is demonstrated in this section using a point solution, as depicted in Figures 2-5. Figure 2 depicts the design of a trajectory transfer from the EM-1 upper stage deployment to lunar capture in a Sun-Earth rotating frame, while Figure 3 portrays a zoomed-in view of the capture phase of the trajectory in an Earth-Moon rotating frame. Figures 4 and 5 display three-dimensional views of the achieved lunar orbit in an inertial Moon centered frame from two different perspectives. This transfer leverages a combination of natural (blue) and low-thrust-enabled (red) arcs to produce motion that is captured around the Moon. For the Lunar IceCube mission, maneuvers are not planned during the first lunar periapsis to allow tracking for a navigation solution during that event since the spacecraft does not have the power capability to both maneuver and use the IRIS-V2 transponder simultaneously. Accordingly, the low-thrust engine is activated after the first lunar flyby. The capture phase of this sample transfer

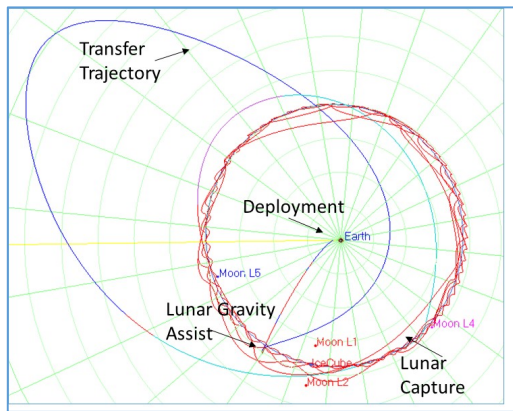


Figure 2. Lunar IceCube trajectory transfer

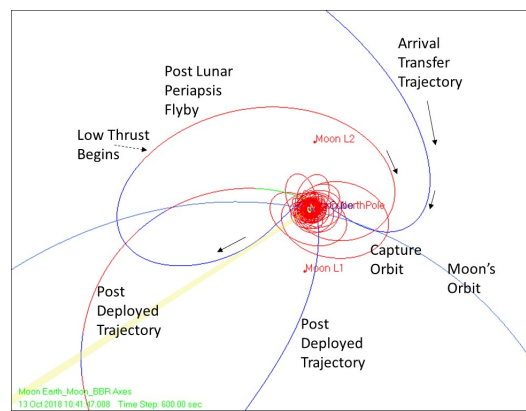


Figure 3. Arrival trajectory in Earth-Moon rotating coordinates

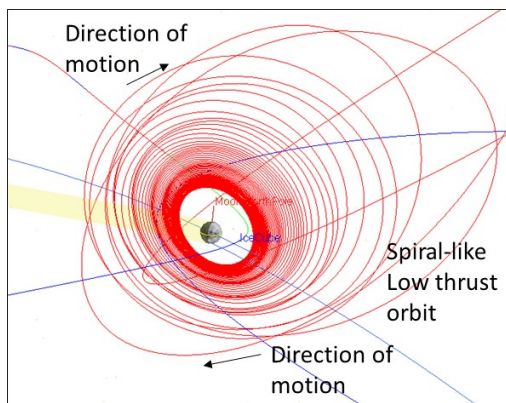


Figure 4. Lunar capture in inertial frame

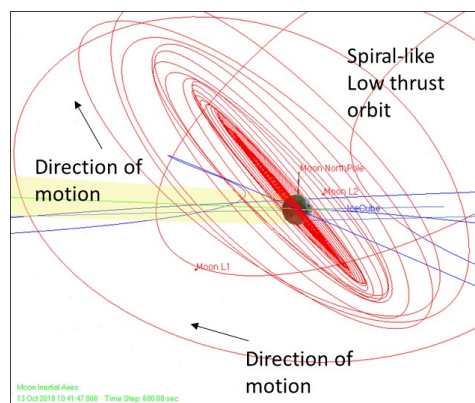
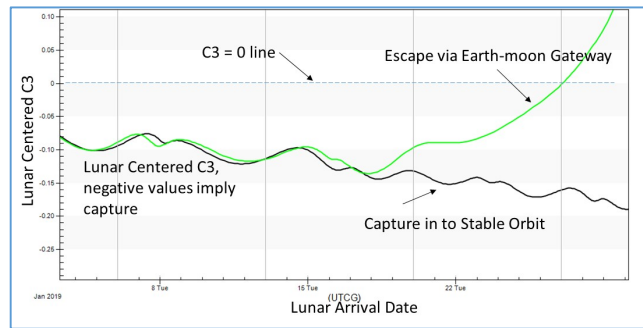


Figure 5. Lunar capture in inertial frame

results in a moderately inclined orbit of approximately 45 deg. Given the limit on the thrust magnitude and, therefore, the capability to adjust the inclination and argument of periapsis, this design does not meet the mission requirements and requires months of maneuvering to adjust the inclination, potentially exceeding the available propellant mass.

In addition to the offset inclination, this sample transfer is particularly sensitive to uncertainty in the incoming lunar arrival conditions and the time at which the low-thrust engine is activated. The sensitivity of this sample path is explored using a measure of the energy: the lunar C3. Consider Figure 6, which displays the lunar C3 as a function of the epoch along the reference path in black, and a perturbed solution in green. This perturbed solution resembles the reference path during the incoming lunar flyby. However, the first thrusting arc is delayed by 2 days. Following this perturbation, subsequent lunar flybys are impacted. Due to the chaotic nature of the multi-body cislunar gravitational environment, this small error results in two distinctly different paths for the remainder of the reference trajectory (red) and perturbed trajectory (blue), as displayed in an Earth-Moon rotating frame in Figure 7. This difference is straightforwardly represented using the lunar C3. In fact, this figure reveals that the sample point solution is contingent on the use of a short duration low-thrust maneuver after entering the Earth-Moon dynamical region to reduce the arrival C3 energy with respect to the Moon. Simultaneously, the Jacobi constant, as computed in the Earth-Moon CR3BP, is also increased. Following a small deviation in the time at which the low-thrust engine is activated, the green curve in Figure 6 demonstrates that such uncertainty can result in the C3 increasing over time to a positive value, indicating that the spacecraft is not captured to the lunar vicinity along the perturbed solution. Such sensitivity in the trajectory following lunar arrival creates significant challenges throughout the trajectory design process. These challenges include obtaining motion that quickly captures into the lunar vicinity and evolves to the required elliptical orbit.



**Figure 6. Comparison of the lunar C3 for two trajectories, a reference path (black) and perturbed solution (green), that differ in the start of the low-thrust maneuver by two days.**

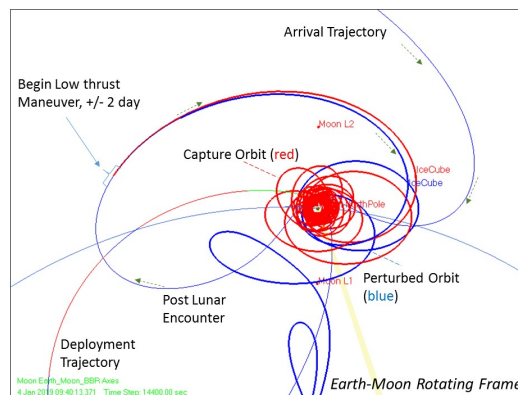


**Figure 7. Sensitivity of arrival energy on a capture trajectory**

## DYNAMICAL SYSTEMS ANALYSIS OF SCIENCE ORBIT APPROACH PATHS

To explore the existence and characteristics of paths that approach the desired lunar science orbit subject to mission constraints on the Keplerian elements, dynamical systems techniques are employed.<sup>12</sup> Given the chaotic nature of the multi-body gravitational environment in cislunar space, such techniques facilitate visualization and identification of candidate motions. In particular, this analysis leverages concepts typically employed in the CR3BP, including the Jacobi constant, libration point gateway analysis, and manifold computation. The resulting insight enables the design of trajectories that reach the desired lunar science orbit given the significant limitations on the propulsive capability of the spacecraft and the incoming path. This analysis is verified via existing point solutions constructed in a high fidelity ephemeris models.

The general behavior of trajectories that approach the desired science orbit with a combination of low-thrust-enabled and natural motion can be split into two phases: a short segment where the multi-body gravitational environment of the Earth-Moon system influences the path; and a longer segment where the lunar gravity serves as the dominant acceleration contribution. In the first segment, concepts from the CR3BP are valuable in exploring the behavior of motion that reaches the lunar vicinity prior to activating the low-thrust engine. This engine is activated throughout the entirety of the second lunar approach segment to provide additional deceleration for the spacecraft to capture into a stable trajectory around the Moon. Throughout both phases of the mission, analysis of feasible capture trajectories is achieved by leveraging a concept similar to manifold computation. In particular, feasible science orbits are discretized and integrated backwards in time using a combination of low-thrust and natural arcs. In a chaotic system, limiting the trajectories of interest to those that are known to capture directly into the desired lunar science orbit in forward time or, equivalently, depart the science orbit in backwards time, reduces the search space. Then, to represent these trajectories, mapping strategies supply a straightforward visualization of a large set of data while also enabling the detection of general trends in the flow. Characterization of the paths that enter the lunar vicinity and evolve into the desired lunar orbit support the development of trajectory design guidelines. To achieve this goal, several aspects of the trajectory design process must be addressed, including: the evolution of the science orbit backwards in time with the low-thrust engine activated close the Moon; determination of the conditions under which the low-thrust engine should be turned off to ensure natural departure through the Earth-Moon  $L_2$  gateway in backwards time; and the formulation of guidelines to translate insight from a backwards time analysis to a set of parameters that can be targeted in forward in time from a constrained lunar approach path.

### Generation of Science Orbit Approach Paths

Paths that approach the science orbit in forward time with the low-thrust engine activated or, equivalently, depart the science orbit in backwards time are computed. Predictions of a lunar orbit have been investigated previously and may be visualized by the rates of Keplerian elements such as the argument of periapsis and eccentricity for initial inclinations.<sup>13</sup> To approximate the Lunar IceCube mission science orbit, the orbital elements are set to  $a = 4287$  km,  $e = 0.5714$ ,  $i = 89$  deg,  $\omega = 0$  deg (i.e. periapsis located over the equator), each fixed by the mission constraints. Feasible science orbits are then generated by varying the right ascension of the ascending node (RAAN) within the range  $\Omega = [0, 360]$  deg, thereby rotating the orbital plane in inertial space. Next, feasible science orbits are discretized by sampling values of the true anomaly,  $\theta^*$ , within the range  $[0, 360]$  degrees. Finally, each state along the orbit supplies an initial condition that can be integrated backwards in time with the low-thrust engine activated.

Although the low-thrust engine could follow an infinite number of possible thrust profiles, some straightforward constraints can reduce the dimensionality of the problem and, thus, the complexity of the design space. In addition to the low-thrust engine possessing a limited thrust magnitude and propellant mass, the total time required to reach the desired science orbit impacts the ability to



begin performing scientific observations. Accordingly, possible thrust profiles for arcs that capture into the desired science orbit in forward time or, equivalently, depart the science orbit in backward time, can be limited heuristically by the total required thrust time. To define this approximate constraint on the thrust profiles modeled in this investigation, consider a Moon-centered Velocity, Normal, Co-Normal (VNC) frame<sup>11</sup>. In this frame, the velocity direction, denoted by the  $\hat{V}$  unit vector is parallel to the inertial velocity vector of the spacecraft relative to the Moon. The co-normal direction,  $\hat{C}$ , is defined normal to the path of the spacecraft, while lying within the orbital plane. Finally, the normal unit vector,  $\hat{N}$ , is perpendicular to the orbital plane and completes the right-handed coordinate system. The engine thrust direction,  $\hat{u}$ , is projected into the VNC coordinates to enable a right-handed physical interpretation. For a thrust vector aligned with the  $\hat{N}$  direction, the primary effect of the additional acceleration is to alter the orientation of the orbital plane. However, the semi-major axis and eccentricity of the orbit are not significantly impacted. Accordingly, it may take an excessively long time for the spacecraft motion to evolve to a low lunar science orbit under the perturbations of the Earth, Moon and Sun gravity as well as the low-thrust engine. Alternatively, orienting the thrust vector solely in the anti-velocity direction, i.e.  $-\hat{V}$ , reduces the velocity magnitude without impacting the direction relative to the Moon. This direct reduction in the velocity magnitude enables the orbit size to be reduced as quickly as possible, essentially reducing the total thrust time. Thus, the reference thrust direction considered within this investigation is aligned with the anti-velocity direction. This constraint on the thrust direction limits the set of feasible capture paths, while also simplifying the trajectory generation and visualization process.

To produce trajectories that capture into the science orbit in forwards time, feasible states that possess various values of the true anomaly for orbits with several values of the RAAN are leveraged as initial conditions in a backwards time integration process. In particular, each state that lies along a feasible science orbit is integrated backwards in time with the low-thrust engine activated in the anti-velocity direction relative the Moon. This long duration maneuver increases the semi-major axis while also impacting the inclination and eccentricity. Such behavior is demonstrated using Figure 8(a), which portrays the natural evolution of an initial condition located at periapsis along a science orbit with a RAAN of 0 degrees at a Modified Julian date (MJD) epoch of 28610 for a spacecraft mass of 13.5 kg. This path, colored blue, closely resembles the original science orbit in size, with the periapsis direction rotating over time. Eventually, after 88 days, the spacecraft impacts the surface of the Moon. However, when the low-thrust engine is activated, as depicted by the red path in Figure 8(b), with the thrust aligned with the anti-velocity direction for 90 days, the orbit grows in size. In addition, the orbital plane slowly shifts with the inclination oscillation about 89 degrees over time. As the trajectory slowly spirals away from the Moon in backward time, the influence of the Earth's gravity increases. Once the spacecraft is sufficiently far from the Moon, the multi-body dynamical environment of the Earth-Moon system dominates the motion of the spacecraft and can supply significant insight into the existence of transfers that depart the lunar vicinity in backwards time, as well as a timeline for deactivating the low-thrust engine.

Due to the chaotic nature of the Earth-Moon system, two slightly perturbed solutions can evolve distinctly differently in backwards time. To demonstrate this concept, consider Figure 9(a) and (b) which depict the path a spacecraft integrated backward in time with the low-thrust vector aligned with the anti-velocity direction from an initial condition along a science orbit at a true anomaly of 40 degrees at an epoch of 28610 MJD. Figure 9(a) begins with a science orbit with RAAN=160 degrees, while Figure 9(b) begins with an orbit at RAAN=180 deg. The chaotic nature of the Earth-Moon system is evident via a comparison between these two figures. Close to the Moon, both trajectories evolve similarly. The semi-major axis increases over time with oscillations with a 13-14 day period, while the eccentricity increases to above 0.5. With the thrust vector oriented in the anti-velocity direction, the RAAN does not change by more than 10 deg over the span of six months. This small deviation in the evolution of the orbital elements is generally dependent on the epoch due to changes in the relative configuration of the Earth, Moon and Sun. In addition, the



Earth acceleration on the spacecraft interacts with the orbital velocity like a maneuver increasing or decreasing the velocity when the orbital plane is parallel to the Moon-Earth direction. These effects impact the eccentricity, thereby altering the rates of the other orbital elements. Once the gravity of the Earth contributes significantly to the motion of the spacecraft, a distinct difference between the two trajectories is apparent: while the trajectory in Figure 9(a) impacts the Moon, the orbit in Figure 9(b) continues to grow in size for 180 days when integrated backward in time.

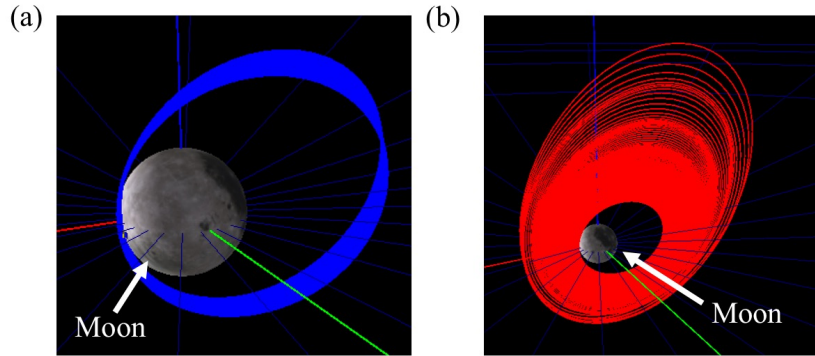


**Figure 8.** (a) Natural motion of a spacecraft backwards in time for 88 days from an initial condition at periapsis along feasible science orbit with RAAN = 0 degrees at an epoch of 28610 MJD, and (b) low-thrust-enabled motion for 90 days backwards in time from the same initial condition.

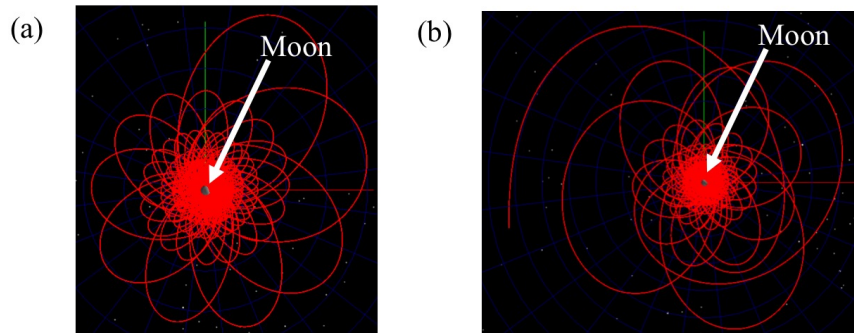


**Figure 9.** (a) Low-thrust-enabled trajectory of a spacecraft integrated backwards in time for nearly six months from an initial condition located at TA=40 degrees along a feasible science orbit with RAAN =160 degrees at an epoch of 28610 MJD, and (b) similar trajectory for RAAN = 180 degrees.

### Lunar Capture Dynamics

Following deployment and an outbound lunar flyby, feasible transfers for the Lunar IceCube spacecraft typically leverage the gravity of the Sun for phasing and energy adjustment to approach a feasible science orbit. Analysis of these trajectories, which connect a state that lies far beyond the lunar radius to a low lunar science orbit, is supported by concepts from multi-body dynamics. In particular, a CR3BP approximation of the Earth-Moon system is valuable. In the CR3BP, the Jacobi constant offers a measure of the energy of the spacecraft, while also placing bounds on the motion.<sup>14</sup> To demonstrate such insight, consider Figure 10, which depicts a zoomed-in view of the Moon in a dimensional Earth-Moon rotating frame. The Moon is located by a cyan-filled circle, while the  $L_1$  and  $L_2$  libration points are depicted as red diamonds. At a value of the Jacobi constant just below

that of the  $L_1$  and  $L_2$  libration points, the gray areas depict forbidden regions bound by the zero velocity curves. The white regions then portray regions in the lunar vicinity where a spacecraft can feasibly travel. For motion that begins outside of the zero velocity curves, a spacecraft can enter the lunar vicinity through the  $L_2$  gateway. Furthermore, for a spacecraft to remain within the lunar vicinity, it must avoid departing through either the  $L_1$  or  $L_2$  gateways. In designing a path for the Lunar IceCube spacecraft, the value of the Jacobi constant for a trajectory entering through the  $L_2$  gateway is constrained by the deployment and post-deployment lunar flyby conditions.

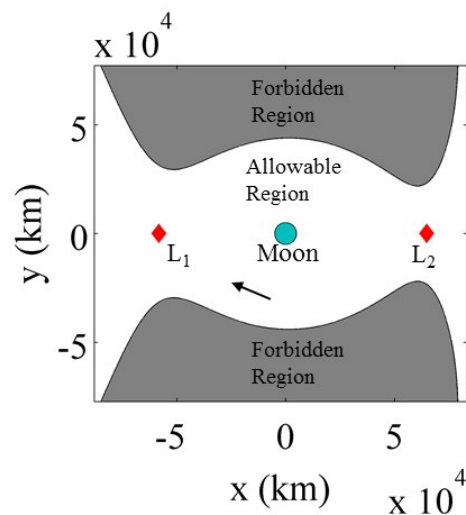


**Figure 10. Earth-Moon gateways and zero velocity curves separating forbidden and allowable regions of motion for a given Jacobi constant.**

A gateway analysis in the Earth-Moon CR3BP enables an exploration of the behavior of the Lunar IceCube spacecraft as it approaches the desired lunar science orbit from beyond the lunar radius. As an example, consider the process described earlier for generating a science orbit approach path: an initial condition along a feasible science orbit is integrated backwards in time with the low-thrust engine activated and thrust direction aligned with the anti-velocity direction. In a CR3BP analysis of this scenario, the value of the Jacobi constant along the science orbit is approximately 4.1. At this Jacobi constant, the  $L_1$  and  $L_2$  gateways are closed and motion cannot escape from the lunar vicinity. When the initial condition is integrated backward in time and the low-thrust engine is activated in the anti-velocity direction, the velocity of the spacecraft increases over time. Simultaneously, the Jacobi constant decreases. In order for the spacecraft to depart through the  $L_2$  gateway and connect to the post-deployment trajectory, the Jacobi constant must be decreased to below that of  $L_2$ , i.e.  $C(L_2) = 3.172$ . This scenario is depicted in Figure 11 (a)-(c) with the Jacobi constant decreasing from left to right. In Figure 11(a), the spacecraft cannot depart from the lunar vicinity in backward time. In Figure 11(c), however, the spacecraft trajectory is energetic enough to connect the lunar science orbit to the post-deployment state. In forward time, the situation can be reversed. To enter the lunar vicinity, the Jacobi constant of the spacecraft in an Earth-Moon system, when located outside the  $L_2$  gateway, must be below  $C(L_2)$  such that the Zero Velocity Curves (ZVCs) resemble Figure 11(c). The spacecraft can naturally pass through the  $L_2$  gateway to perform at least one lunar flyby while orbit determination is performed. Once an accurate navigation solution is obtained, the low-thrust engine may be activated in the anti-velocity direction to decrease spacecraft velocity and increase the Jacobi constant, thereby closing the  $L_2$  gateway. This scenario is depicted in Figure 11(b). As the low-thrust engine remains activated and the Jacobi constant increases even further, the  $L_1$  gateway closes, effectively rendering the spacecraft captured in the lunar vicinity. With the Jacobi constant continuing to increase to a value of 4.1, the allowable region in the vicinity of the Moon reduces in size and the spacecraft orbit shrinks. Such insight into the desired energy profile, based on a multi-body dynamical analysis, provides a general itinerary for the science orbit approach path.

To search the design space for operationally feasible science orbit approach paths via backwards time integration, the Earth-Moon CR3BP gateway analysis is leveraged to guide the construction of the trajectory generation process<sup>10</sup>. Specifically, each initial condition located at a given true anomaly along a feasible science orbit is integrated backwards in time in a point mass ephemeris model with the thruster activated in the anti-velocity direction until a Jacobi constant equivalent to that of  $L_1$  is achieved.

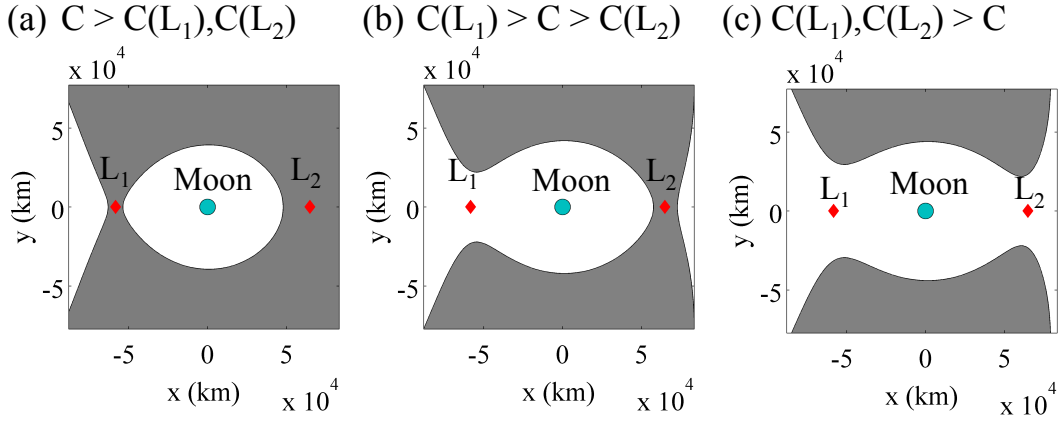


**Figure 11. Evolution of the zero velocity curves and opening of the  $L_2$  gateway as  $C$  is decreased.**

With the thruster still active, the trajectory is integrated further until the subsequent apse (periapsis or apoapsis). From this state, the spacecraft is naturally propagated backwards in time (i.e. the thruster is not activated) until it reaches the  $L_1$  or  $L_2$  gateways, impacts the Earth or until a maximum integration time. The parameters describing this trajectory are stored and considered operationally feasible if they pass through the  $L_2$  gateway and encounter an apogee beyond the lunar radius within 50 days. This process is then repeated by integrating backwards in time with the low-thrust engine activated to the next apse until the trajectory impacts or departs the Earth vicinity. A sample trajectory sequence is displayed in Figure 12 for the prescribed values of  $a$ ,  $e$ , and  $i$ , a final epoch of 28601 MJD, a final mass of 13.5 kg, a RAAN of 150 degrees and a true anomaly of 135 degrees. This sample trajectory is visualized in (a) a Moon-centered inertial J2000 equatorial frame and (b) a Moon-centered Earth-Moon rotating frame. In both plots, green indicates thrusting segments while blue curves identify natural coasting arcs. In this example, the low-thrust engine causes the orbit to increase in size until the gravity of the Earth contributes significantly to the total acceleration acting on the spacecraft. Then, the trajectory follows a path predicted by the Earth-Moon CR3BP to depart through the  $L_2$  gateway in backward time. In forward time, this path presents a feasible trajectory for the spacecraft from a post-deployment state to the lunar science orbit.

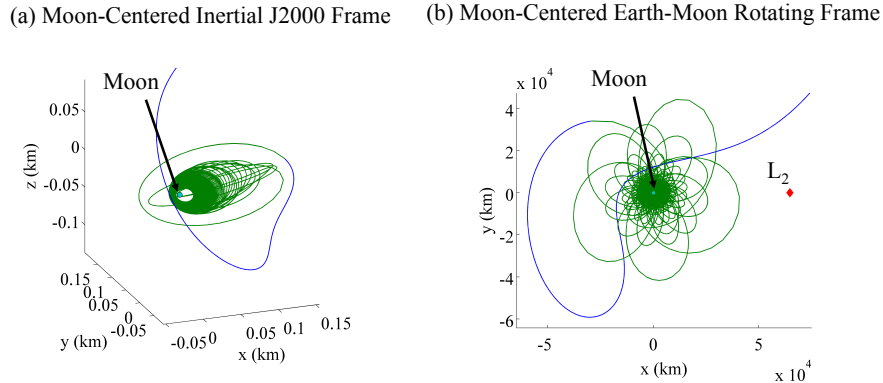


**Figure 12. Sample arc that captures into the desired lunar science orbit, displayed in (a) a Moon-centered inertial J2000 equatorial frame, and (b) a Moon-centered Earth-Moon rotating frame. Green arcs indicate that the thruster is activated in the anti-velocity direction, while blue arcs correspond to natural motion**

For feasible science approach paths, each of the apses at which the low-thrust engine is first activated, after the spacecraft has entered the lunar vicinity, must lie close to the unstable manifold of an  $L_2$  libration point orbit as predicted by the CR3BP. States that lie within these manifolds pass

through the  $L_2$  gateway prior to evolving towards the lunar vicinity.<sup>12</sup> Since a wide variety of periodic and quasi-periodic orbits exist within the  $L_2$  vicinity, computing the set of all unstable manifolds corresponding to  $L_2$  libration point orbits may be cumbersome and computationally expensive. Alternatively, a surface of section may be defined just beyond the x-coordinate of  $L_2$ . Then, position coordinates in the y- and z- directions are seeded on this hyperplane. To complete the definition of states that produce trajectories passing through the  $L_2$  gateway, a velocity vector is defined. For each combination of position variables,  $(x,y,z)$ , several velocities are defined to possess a negative x-component, with the relative values of the y- and z-components then varied. Only the magnitude of the velocity vector is constrained to ensure a fixed value of the Jacobi constant across the set of initial conditions. Then, these states are integrated forward to their first periapsis; any trajectories that impact the Moon are discarded. Figure 13(a) depicts a sample set of periapses, in purple, corresponding to trajectories that pass through the  $L_2$  gateway, i.e., the unstable manifolds of  $L_2$  periodic and quasi-periodic orbits at a Jacobi constant of  $C = 3.138$ . The Moon is located by a cyan circle. In backwards time, any trajectory with a periapsis that falls within the unstable manifold of an  $L_2$  orbit immediately departs through the  $L_2$  gateway. For values of the Jacobi constant below that of  $L_2$ , these periapses tend to lie in the top left quadrant of the Earth-Moon rotating frame. Accordingly, trajectories that do not possess a periapsis within the top left quadrant of the Moon-centered Earth-Moon rotating frame do not naturally depart through the  $L_2$  gateway in backward time. Of course, the location of periapses or apoapses for subsequent crossings of the  $L_2$  periodic and quasi-periodic orbit unstable manifolds tend to stretch in the phase space, complicating visualization and the development of any heuristic guidelines for shutting off the thruster in backward time. Nevertheless, such insight from the CR3BP is valuable in exploring the existence of trajectories that enter naturally through the  $L_2$  gateway prior to evolving towards the desired lunar science orbit under the influence of the low-thrust engine. In fact, in backward time, the low-thrust engine is deactivated at an apse that lies within the unstable manifold of an  $L_2$  periodic or quasi-periodic orbit and, therefore, the subsequent motion naturally passes through the  $L_2$  gateway.

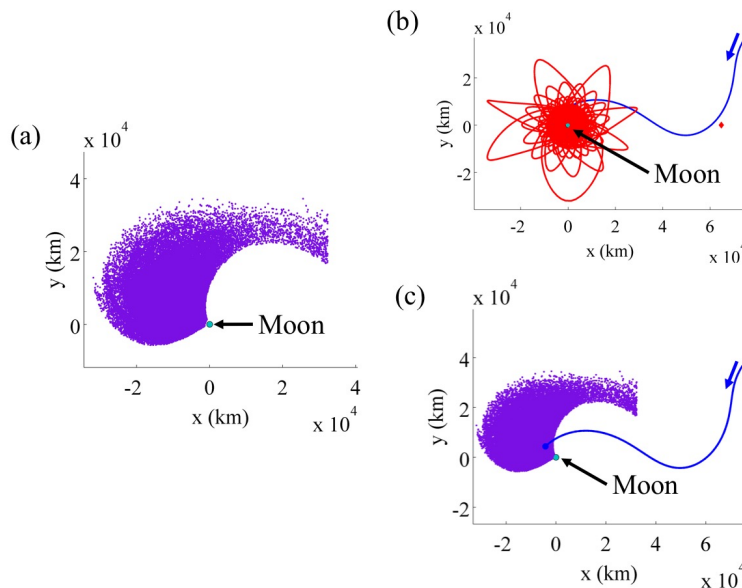


**Figure 13. Demonstration of natural manifold structures enabling flow towards the lunar vicinity through (a) the first periapses of the unstable manifolds of the  $L_2$  periodic and quasi-periodic orbits, (b) a sample science orbit approach trajectory where the low-thrust engine is activated at the first perilune, and (c) the location of this perilune overlaid on the unstable manifold periapses.**

An example of a science orbit approach trajectory, generated in a point mass ephemeris model, which follows this itinerary within the lunar vicinity, appears in Figure 13(b). The red arcs along this transfer indicate low-thrust-enabled motion while the blue arcs correspond to natural motion. A red diamond locates  $L_2$  while a cyan circle indicates the location of the Moon. The low-thrust engine is activated, in forward time, at the first perilune following entrance to the lunar vicinity from the  $L_2$  gateway. This natural leg over the science approach trajectory is overlaid on the first periapses of the unstable manifolds of the  $L_2$  periodic and quasi-periodic orbits in Figure 13(c). The first perilune is depicted as a blue-filled circle, and lies within the unstable manifold region in the top left quadrant of the Earth-Moon rotating frame.

### Visualization of Science Orbit Approach Paths

To visualize the set of trajectories which approach the desired science orbit in forward time or, equivalently, depart the orbit in backward time with the low-thrust engine activated prior to passing through the  $L_2$  gateway naturally, mapping strategies are employed. In particular, a surface of section is defined using an x-coordinate that lies just beyond the  $L_2$  libration point. This surface of section is depicted in the planar projection in Figure 14, with the Moon indicated by a cyan circle and the libration points located via red diamonds. The surface of section is displayed with a blue dashed line. Given this surface of section definition, each of the science orbit approach paths are integrated backward in time from the initial condition along the low lunar orbit with the low-thrust engine activated. At each periapsis or apoapsis with a Jacobi constant below that of  $L_2$ , the spacecraft is naturally propagated until it reaches the defined surface of section. The crossing of each trajectory with this surface of section is recorded and plotted on a map. Additional information such as the spacecraft mass, epoch and Jacobi constant at the crossing of the hyperplane are also useful. The Jacobi constant is employed as the energy measurement of the Earth-Moon three body system (or in some cases the lunar centered C3 orbital energy) and the velocity magnitude and direction help define target regions of interest that may achieve a polar orbit.

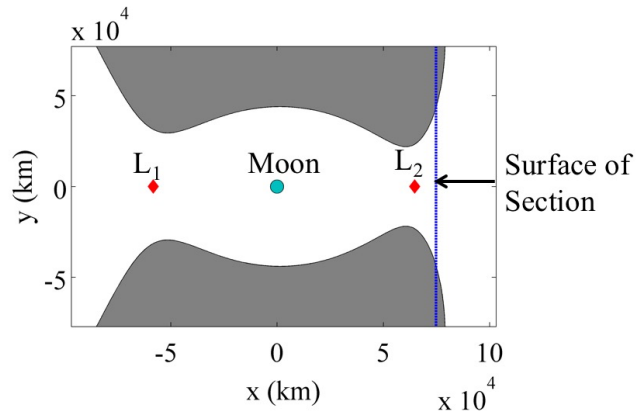


**Figure 14. Definition of the surface of section used to construct an  $L_2$  gateway map.**

As an example of an  $L_2$  gateway map that captures motion that evolves towards the desired lunar orbit, consider the developed procedure for generating science orbit approach paths. This procedure is implemented for orbits with a RAAN in the range  $[0, 360]$  in increments of 20 degrees, and initial conditions seeded along each orbit in increments of 20 degrees. The final spacecraft mass along the science orbit is set equal to 13.5 kg, while the final epoch is varied between 28610 MJD and 28630 MJD in increments of a day. Science orbit approach arcs are generated using a combination of low-thrust-enabled and natural motion, with each crossing of the surface of section recorded and plotted on the  $L_2$  gateway map. Of course, the information describing each state is multi-dimensional. However, to simplify visualization, only a subset of the state information is represented on a two-dimensional map. Sample maps appear in Figure 15(a) and (b). In each figure, the crossing of each feasible science orbit approach arc with the surface of section is represented by its y- and z-coordinates in an Earth-Moon rotating frame. Then, each point is colored in Figure 15(a) by the Jacobi constant as measured in the Earth-Moon rotating frame and in Figure 15(b) by the time of flight to the  $L_2$  gateway crossing in days. Each of the crossings of these maps tends to possess a velocity that is directed in the -x direction and the -y direction. Analysis of these two figures reveals

that there are two types of trajectories that approach the desired polar science orbit: one set that possesses a low Jacobi constant (blue points in Figure 15(a)) and longer time of flight (cyan to red points in Figure 15(b)), and one set of trajectories that possesses a higher Jacobi constant (red points in Figure 15(a)) and a shorter time of flight (blue points in Figure 15(b)) to the  $L_2$  gateway. An example of each of these trajectories appears in Figure 16(a) and (b), respectively, in an Earth-Moon rotating frame with blue arcs indicating natural motion and red curves locating low-thrust-enabled segments.

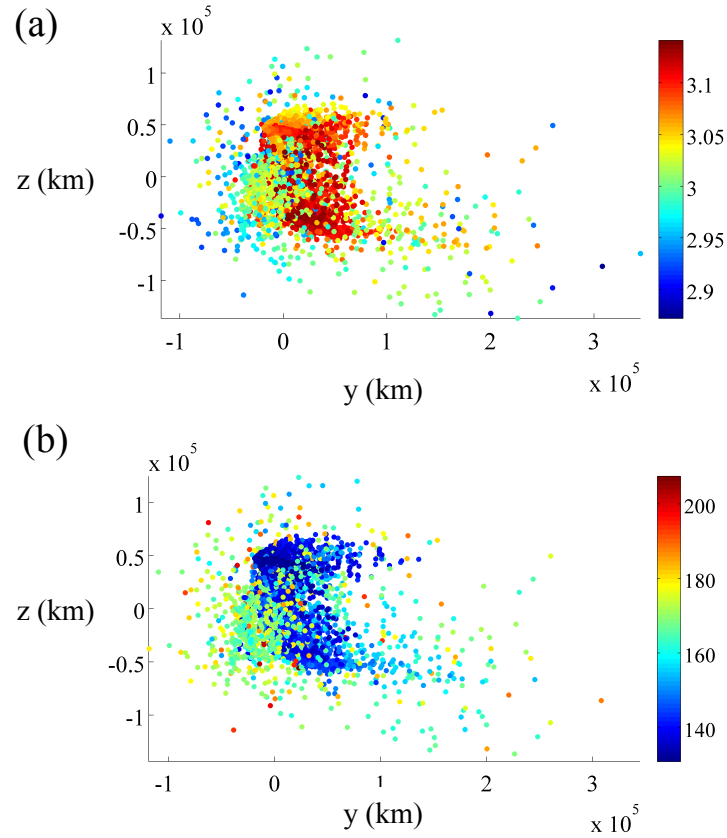


**Figure 15.  $L_2$  gateway map depicting crossings of trajectories that arrive at the lunar science orbit in with the assistance of a low-thrust engine at epochs between 28610 MJD and 28630 MJD, colored by (a) Jacobi constant in the Earth-Moon CR3BP and (b) time of flight to the hyperplane crossing.**

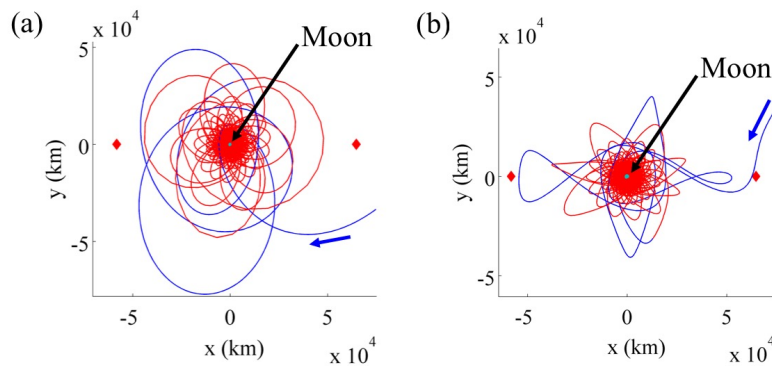


**Figure 16. Sample science orbit approach trajectories with (a) low Jacobi constant value and long time of flight, and (b) high Jacobi constant value and short time of flight.**



The constructed maps offer  $L_2$  gateway crossing conditions that may be used in the trajectory design process to guide the targeting process to achieve a trajectory that evolves to a lunar polar orbit with the assistance of the low-thrust engine. Selection of feasible state components from this map is dependent on the value of the Jacobi constant at arrival. Specifically, the final phase of the Lunar IceCube transfer trajectory is dependent on the outgoing EM-1 launch and deployment parameters that yield an overall lunar arrival energy level, thereby constraining the Jacobi constants of feasible map crossings of trajectories that reach the desired lunar orbit. Recall, however, that each crossing of the map occurs at a specific epoch and for a specific mass of the spacecraft. Rather than iteratively constructing additional maps for the desired epoch at the map crossing, the single map in Figure 15 may be useful. Consider a fixed incoming approach path which passes through the  $L_2$  gateway close to one of the crossings on the map in Figure 15. However, the epoch of this map crossing and the epoch of the point solution at its intersection with the  $L_2$  gateway hyperplane differ by 2 days. The state information for this nearby crossing can be used to find a similar trajectory that results in nearly polar motion about the Moon by leveraging a multiple shooting corrections scheme. This corrections scheme uses as an initial guess the trajectory and thrust profile corresponding to a given map crossing, and iteratively updates a sequence of states distributed along the trajectory as well as the corresponding epochs and, if applicable, thrust directions. With each update in the corrections scheme this information is varied until a similar trajectory is found with a map crossing at the same position coordinates, as expressed in an Earth-Moon rotating frame, but a new epoch. To demonstrate the persistence of these transfers for alternate epochs and, therefore, the value in using a mapping strategy to capture the general trends of the flow through the  $L_2$  gateway, consider the sample transfer in Figure 17(a). Recall that blue arcs indicate natural motion while red curves indicate low-thrust-enabled arcs. This trajectory appears in a Moon-centered Earth-Moon rotating frame. The map crossing corresponding to this trajectory occurs at an epoch of 28433 MJD, with a Jacobi constant of 3.13, eventually evolving into a science orbit with a RAAN of 20 degrees and reaching the orbit at apoapsis. At the map crossing, the mass of the spacecraft is equal to 13.7 kg. A corrections algorithm is applied to this path to find a similar trajectory at an  $L_2$  gateway arrival epoch 2 days later, i.e. 28435 MJD. The reference path in Figure 17(a) is discretized into 150 nodes along the first 80 days of the 130-day trajectory – subsequent analyses with higher fidelity models of the Moon can determine a complete science orbit approach path. The goal in this investigation is simply to find a nearby trajectory with nearly polar motion towards the end of the 80-day transfer. The corrections process yields the trajectory depicted in Figure 17(b) and resembles the original reference path.

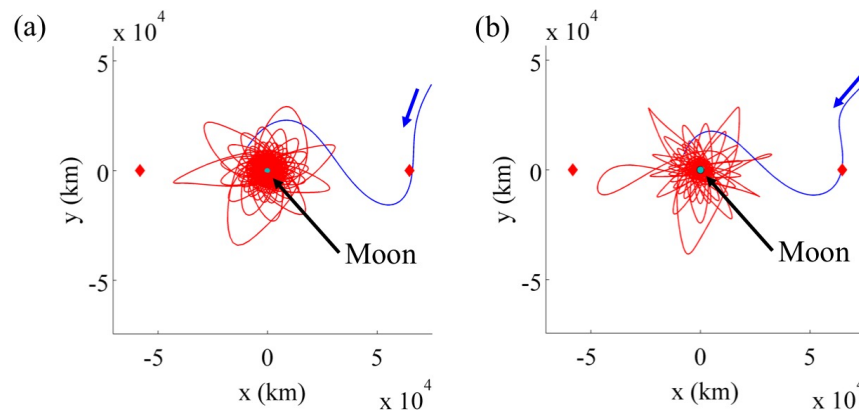


**Figure 17. Recovery of lunar approach paths from  $L_2$  gateway map at (a) an epoch of 28433 MJD and (b) two days later at an epoch of 28435 MJD. Trajectories appear in an Earth-Moon rotating frame with blue arcs indicating natural motion and red arcs indicating low-thrust-enabled motion.**

These trajectories possess identical position components of the  $L_2$  gateway map crossing, while the velocity differs by approximately 33 m/s in magnitude. Note that the velocity vector at the  $L_2$



gateway crossing were not constrained. Furthermore, without directly constraining the orbital elements along the first 80 days along this path, the inclination only varies by five degrees. Higher fidelity modeling and subsequent corrections of the entire path along the science orbit approach arc can be used in future analyses to recover exact polar motion. Nevertheless, the produced map supports the identification of general trends in the flow and, in combination with a corrections algorithm, the location of science orbit approach paths at a variety of epochs, even those not directly represented on the map.

## COMPARISON TO EXISTING POINT SOLUTIONS

Visualization of the natural flow through the Earth-Moon  $L_2$  gateway and subsequent low-thrust-enabled capture via dynamical systems techniques is also useful in analysis of existing point solutions. These point solutions, constructed in an operational high-fidelity model, include transfers that reach a variety of inclinations. First, consider a path that reaches a 93 degree inclination low altitude lunar orbit, as portrayed in Figures 18-21 from deployment to lunar capture. Figure 18 portrays the cruise segment in a Sun-Earth rotating coordinate frame where the trailing edge lunar flyby is augmented to permit the one-loop design using the solar influence to change the periapsis radius to the lunar orbit radius. Figure 19 presents the arrival and capture trajectory in an Earth-Moon rotating frame and shows the inbound surface of section crossings. Figures 20 and 21 displays the captured orbit in a Moon-centered inertial frame. Note that, even with the identification of arrival or gateway surface of section location, low-thrust directional maneuvers may be necessary to attain the precise orbital element requirements. This additional acceleration can be leveraged to achieve both a stable, two-body like lunar orbit, and the proper orientation of the orbital plane.

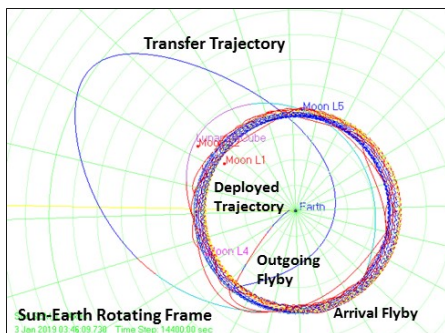


Figure 18. Transfer in Sun-Earth rotating frame

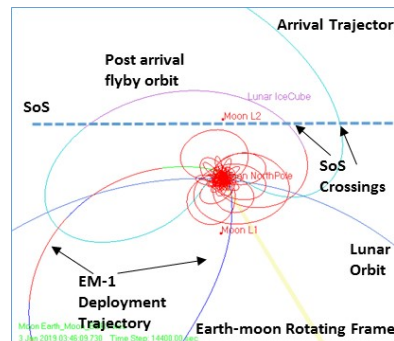


Figure 19. Transfer in Earth-Moon rotating frame

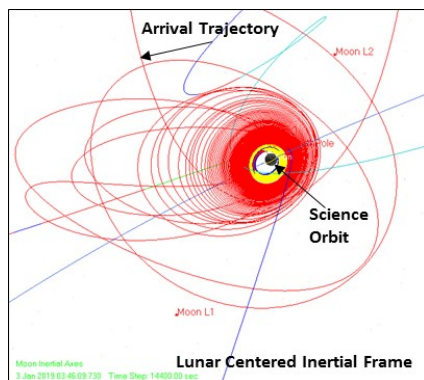


Figure 20. Transfer to science orbit-side view

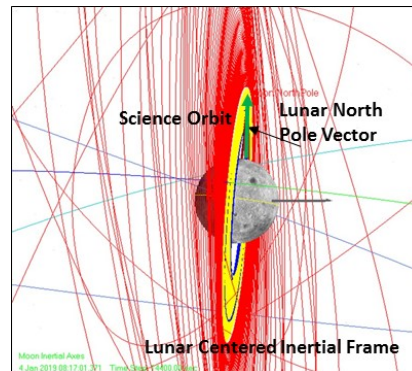
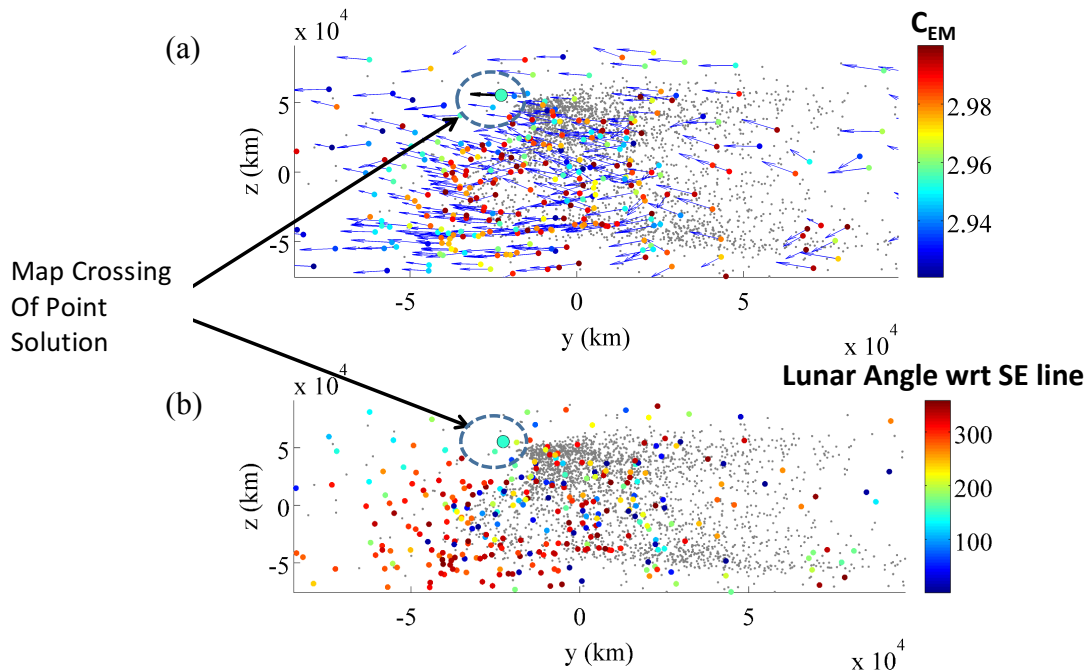


Figure 21. Transfer to science orbit showing polar Orbit

A trajectory that is evolving into a stable lunar orbit, but with a small error in inclination or argument of periapsis can be modified by biasing the low-thrust system's thrust vector with respect to the anti-velocity vector and the low-thrust magnitude. Nevertheless, this point solution results in motion that is captured into the lunar vicinity, with a 93 degree inclination. Accordingly, the lunar approach segment along this solution can be compared to the  $L_2$  gateway map for verification.

To confirm the observations produced via an analysis of the lunar approach dynamics, a sample trajectory, simulated using operational high fidelity tools, is compared to the  $L_2$  gateway map. Figures 22(a) and (b) depict the map crossings for trajectories that achieve near polar orbits for a selected set of epoch values. In particular, only crossings with a similar Jacobi constant to the crossing of the hyperplane along the sample solution are colored. The remaining crossings are colored gray. In Figure 22(a), each crossing is colored by its Jacobi constant with vectors indicating the  $y$ - and  $z$ -components of velocity at the hyperplane. Figure 22(b) depicts the same map information with each crossing colored by the angle of the Moon measured counterclockwise from the  $+x$  direction in the Sun-Earth rotating frame. The map crossing marked by a large cyan circle represents the existing point solution, generated in a high fidelity operational modeling environment, which yields a stable lunar orbit with an inclination of 93 degrees. Although the epoch of the map crossings may differ, this simulated trajectory is described by a Jacobi constant and lunar angle at the crossing of the hyperplane in the  $L_2$  gateway that is similar to that of nearby map crossings. Nearby the sample point solution, represented with a large cyan circle and black velocity vector, the velocity vectors for crossings with a similar position, Jacobi constant and lunar angle are pointed in a similar direction. Thus, the map crossing associated with the sample solution, producing nearly polar motion, falls in a region of the map where crossings occur and possesses a similar energy, lunar angle and velocity direction.



**Figure 22. Comparison of  $L_2$  gateway map, colored by (a) Jacobi constant measured in the Earth-Moon system and (b) lunar angle, and a sample point solution that reaches a 93 degree inclination lunar orbit displayed as a large circle. Vectors indicate  $y$ - and  $z$ - velocity components.**

The  $L_2$  gateway maps constructed in this investigation also support the analysis of problematic lunar approach arcs, i.e. those that do not reach a polar lunar orbit. Consider, for instance, a point solution that results in captured motion described by an inclination of 45 degrees. A zoomed-in view of this trajectory in the lunar vicinity appears in Figure 3, relative to an Earth-Moon rotating

frame. Upon reaching a low lunar orbit, the thrust vector could be oriented in the direction of the orbit normal to shift the orbital plane. However, due to the limited thrust magnitude of the BIT-3 engine, this orbital maneuver would require an excessively long thrust time and, potentially, exceed the available propellant mass. Figure 23 depicts the map crossings for trajectories that achieve near polar orbits for a selected set of epoch values, colored by their Jacobi constant using the guidelines established earlier. The map crossing marked by a cyan-filled square represents the existing point solution, generated in a high fidelity operational modeling environment, which yields a stable lunar orbit with an inclination of 45 degrees. This map crossing represents the last intersection of the point solution with the hyperplane. Comparison of the map crossing associated with this point solution to the nearby map crossings reveals that this last hyperplane crossing occurs in a region where there are few cyan points and a large grouping of red and orange points, corresponding to a significantly higher value of the Jacobi constant. The scarcity of map crossings at a similar energy level in the vicinity of this point solution may indicate increased difficulty or sensitivity in attaining a polar orbit from the white region in the  $L_2$  gateway map. In fact, it appears that, in the vicinity of the point solution on the  $L_2$  gateway map, feasible transfers occur for a lower energy or higher Jacobi constant.

Using the  $L_2$  gateway map information, the trajectory designer may employ the low-thrust engine prior to lunar approach to shift the crossing of the hyperplane to another region on the  $L_2$  gateway map. Specifically, these map crossings can be used in conjunction with an additional low-thrust arc to construct a discontinuous initial guess. This guess is then corrected via a multiple shooting algorithm to identify a continuous trajectory that reaches a feasible lunar science orbit from the constrained lunar approach conditions along the sample point solution.<sup>10,11</sup> Consider, for example, the cyan colored map crossing indicated in Figure 23 by the label “pick new science approach arc”. The corresponding trajectory possesses a similar value of the Jacobi constant at the  $L_2$  gateway as the point solution, and can be employed to construct a discontinuous initial guess. The corresponding science orbit approach arc is combined with the existing point solution, which is trimmed to begin at the first crossing of the  $L_2$  hyperplane, occurring approximately 21 days before the crossing overlaid on the  $L_2$  gateway map. The initial condition corresponding to this first  $L_2$  hyperplane crossing is then held constant to preserve the post-deployment portion of the point solution. Approximately 10.5 days after this new initial condition, three low-thrust-enabled arcs within a 10 day interval, are introduced to modify both the position and velocity of the second  $L_2$  hyperplane crossing on the gateway map. Then, the science orbit approach arc corresponding to the crossing selected from the  $L_2$  gateway map is appended to the end of the point solution and discretized, with the epoch and spacecraft mass at each node modified to artificially enforce continuity in these two variables. While the discretized arcs along the science orbit approach path no longer form a continuous solution, they can be corrected to recover a nearby continuous solution with a relatively similar geometry that also connects to the incoming approach arc along the existing point solution. To achieve these corrections, a multiple shooting algorithm is constructed in a low-thrust-enabled point mass ephemeris model of the Sun, Earth and Moon.<sup>10</sup> Although the initial condition along this solution is held constant to match the point solution, the orbital elements at the end of the lunar approach phase are allowed to vary. After application of this differential corrections scheme, a continuous solution, depicted in Figure 24, is recovered. This solution is plotted in (a) a Sun-Earth rotating frame and (b) Moon Inertial MJ2000 frame with red arcs indicating segments where the low-thrust engine is activated, while natural arcs are colored blue. This corrected trajectory approaches a low altitude lunar orbit with an inclination of 95 degrees, which may be corrected to a value of 90 degrees in a higher fidelity model of the lunar gravitational field. The construction of this new solution demonstrates the utility of the  $L_2$  gateway map information in recovering a nearly polar science orbit approach path from a constrained incoming path.

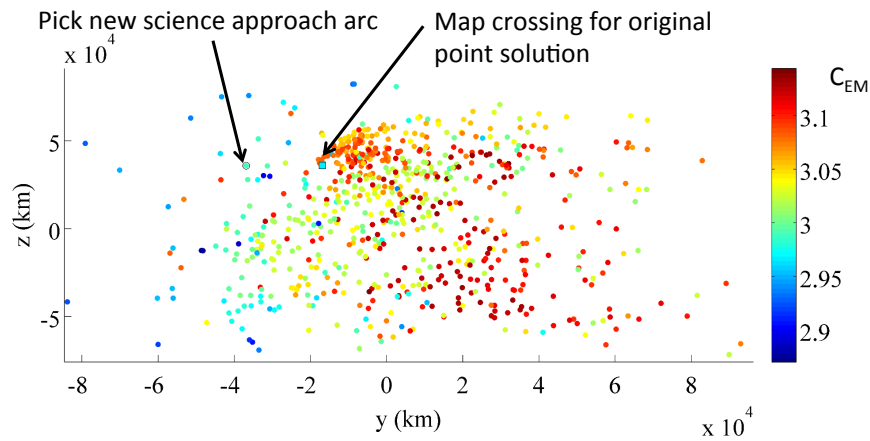


**Figure 23.**  $L_2$  gateway map, colored by Jacobi constant measured in the Earth-Moon system, with the crossing of a sample point solution that reaches a 45 degree inclination lunar orbit overlaid. An additional crossing, leveraged to alter the point solution, is also indicated.

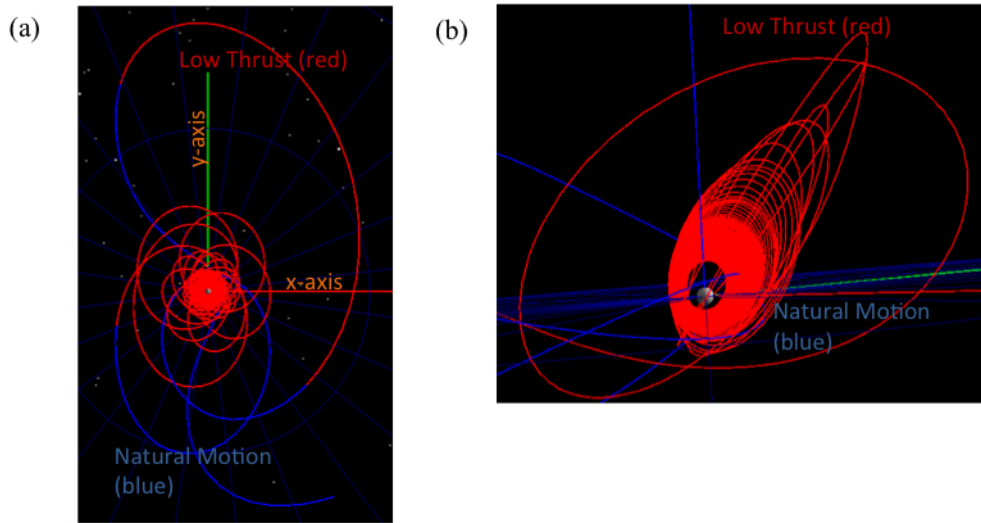


**Figure 24.** Sample point solution, corrected from a discontinuous initial guess, to achieve nearly polar motion. Solution displayed in (a) a Sun-Earth rotating frame and (b) a Moon Inertial MJ2000 frame with red arcs indicated low-thrust enabled motion and blue arcs locating natural segments.

## CONCLUSIONS

The described trajectory design procedure leverages dynamical system theory to explore the existence and itinerary of transfers to a stable, polar lunar orbit from a higher energy approach path. This process employs techniques from the CR3BP, in combination with high fidelity models, to generate trajectories that evolve to a low altitude lunar orbit via backwards integration. These feasible science orbit approach arcs are then visualized and characterized via the application of mapping strategies. This process is verified by comparison to existing point solutions constructed in operational-level modeling software. This investigation addresses the challenges associated with designing such multi-body transfers into stable lunar orbits limited by a low-thrust system. By leveraging CR3BP information, such as the Jacobi constant and mapping techniques, a transfer that links the high-energy deployment trajectories to a feasible lunar science orbit can be constructed. This process is demonstrated via an existing point solution, which originally approaches a 45-degree inclination orbit, and is altered using information from an  $L_2$  gateway map to achieve nearly polar motion about the Moon.

## ACKNOWLEDGMENTS

This work was completed at NASA Goddard Space Flight Center and at Purdue University under NASA Grants NNX13AM17G, NNX16AT688A, and NNX16AM40H. The authors wish to thank Purdue University's School of Aeronautics and Astronautics and the College of Engineering, as well as the Zonta International Amelia Earhart Fellowship.

## REFERENCES

- <sup>1</sup> G. Norris, "Secondary Payloads Overview", Accessed January 2016 at: <https://www.nasa.gov/sites/default/files/files/Secondary-Payloads-Overview-Rev2.pdf>
- <sup>2</sup> Spacedaily.com, "Space Launch System to Boost Science with Secondary Payloads" Accessed January 2016 at: [http://www.spacedaily.com/reports/Space\\_Launch\\_System\\_to\\_Boost\\_Science\\_with\\_Secondary\\_Payloads\\_999.html](http://www.spacedaily.com/reports/Space_Launch_System_to_Boost_Science_with_Secondary_Payloads_999.html).
- <sup>3</sup> D. Folta, M. Woodard, K.C. Howell, C. Patterson, W. Schlei, "Applications of Multi-Body Dynamical Environments: The ARTEMIS Transfer Trajectory Design," *Acta Astronautica*, Vol. 74, 2012, pp. 237-249.
- <sup>4</sup> P.E. Clark, B. Malphrus, R. MacDowall, D. Folta, A. Mandell, C. Brambora, D. Patel, S. Banks, K. Hohman, V. Hruby, K. Brown, J. Kruth, R. Cox, "Lunar Ice Cube: Determining Volatile Systematics Via Lunar Orbiting Cubesat," *European Planetary Science Congress 2015*, Vol. 10.
- <sup>5</sup> D. Folta, N. Bosanac, A. Cox, K.C. Howell, "The Lunar IceCube Mission Design: Construction of Feasible Transfer Trajectories with a Constrained Departure," AAS/AIAA Space Flight Mechanics Meeting, Napa Valley, CA, February 2016.
- <sup>6</sup> Busek.com, "3cm RF Ion Thruster" Accessed January 2016: [http://www.busek.com/index\\_htm\\_files/70010819%20RevA%20Data%20Sheet%20for%20BIT-3%20Ion%20Thruster.pdf](http://www.busek.com/index_htm_files/70010819%20RevA%20Data%20Sheet%20for%20BIT-3%20Ion%20Thruster.pdf).
- <sup>7</sup> Haapala, A., Vaquero, M., Pavlak, T., Howell, K., and Folta, D., "Trajectory Selection Strategy for Tours in the Earth-Moon System," AAS/AIAA Astrodynamics Specialist Conference, Hilton Head, SC, August 10-15, 2013.
- <sup>8</sup> General Mission Analysis Tool. Available: [gmtcentral.org](http://gmtcentral.org). Software package, 2016.
- <sup>9</sup> Systems Tool Kit, Software Package, Analytical Graphics Inc., 2016.
- <sup>10</sup> N. Bosanac, A. Cox, K.C. Howell, D. Folta, "Trajectory Design for a Cislunar CubeSat Leveraging Dynamical Systems Techniques: The Lunar IceCube Mission", AAS/AIAA Space Flight Mechanics Meeting, San Antonio, TX, February 2017.
- <sup>11</sup> N. Bosanac, "Leveraging Natural Dynamical Structures to Explore Multi-Body Systems," PhD Dissertation, School of Aeronautics and Astronautics, Purdue University, West Lafayette, IN, August 2016.
- <sup>12</sup> A. Haapala, "Trajectory Design Using Periapse Maps and Invariant Manifolds," M.S Thesis, School of Aeronautics and Astronautics, Purdue University, West Lafayette, IN, December 2010.
- <sup>13</sup> D. Folta, D. Quinn, "Lunar Frozen Orbits", AAS/AIAA Astrodynamics Specialist Conference, Keystone, CO, August, 2006
- <sup>14</sup> S. Wiggins, C.J. Wiesenfeld, T. and Uzer, "Impenetrable Barriers in Phase-Space," *Physical Review Letters*, 86:5478-5481, June 2001